JOURNAL OF BACTERIOLOGY, May 2010, p. 2613–2623 Vol. 192, No. 10
0021-9193/10/$12.00 doi:10.1128/JB.01605-09

Overlapping Alternative Sigma Factor Regulons in the Response to Singlet Oxygen in *Rhodobacter sphaeroides*▽†

Aaron M. Nuss, Jens Glaeser,* Bork A. Berghoff, and Gabriele Klug

Institut für Mikrobiologie und Molekularbiologie, Universität Giessen, Heinrich-Buff-Ring 26, D-35392 Giessen, Germany

Received 10 December 2009/Accepted 9 March 2010

Organisms performing photosynthesis in the presence of oxygen have to cope with the formation of highly reactive singlet oxygen ($^1O_2$) and need to mount an adaptive response to photooxidative stress. Here we show that the alternative sigma factors $RpoH_I$ and $RpoH_{II}$ are both involved in the $^1O_2$ response and in the heat stress response in *Rhodobacter sphaeroides*. We propose $RpoH_{II}$ to be the major player in the $^1O_2$ response, whereas $RpoH_I$ is more important for the heat stress response. Mapping of the 5′ ends of $RpoH_{II}$- and also $RpoH_I$/$RpoH_{II}$-dependent transcripts revealed clear differences in the −10 regions of the putative promoter sequences. By using bioinformatic tools, we extended the $RpoH_{II}$ regulon, which includes genes induced by $^1O_2$ exposure. These genes encode proteins which are, e.g., involved in methionine sulfoxide reduction and in maintaining the quinone pool. Furthermore, we identified small RNAs which depend on $RpoH_I$ and $RpoH_{II}$ and are likely to contribute to the defense against photooxidative stress and heat stress.

Rhodobacter sphaeroides 2.4.1 induces the photosynthetic apparatus when the oxygen tension in the environment decreases in order to perform anoxygenic photosynthesis. In the presence of oxygen and light, *R. sphaeroides* still grows well even when photosynthetic pigments are highly abundant in the cell. Bacteriochlorophylls and their precursors can act as photosensitizers, causing the formation of highly toxic reactive singlet oxygen ($^1O_2$). Carotenoids prevent the formation of $^1O_2$ by quenching excited bacteriochlorophyll molecules and by direct quenching of $^1O_2$ (7, 10). However, *R. sphaeroides* needs to mount an adaptive response to $^1O_2$ exposure that does not depend on carotenoids (2, 10).

Alternative sigma factors represent important regulatory systems, which control gene expression in bacteria under diverse stress conditions. It was shown earlier that the extracytoplasmic function (ECF) sigma factor RpoE is a major player in the $^1O_2$ stress response in *R. sphaeroides* (2). Dissociation of RpoE from its anti-sigma factor ChrR leads to the activation of genes involved in the response to $^1O_2$ (1, 2). Only recently we demonstrated that the expression of *rpoH*$_{II}$, a gene encoding an alternative sigma factor of the σ^{32} family, directly depends on RpoE, forming a sigma factor cascade (22). $RpoH_{II}$ (σ^{38}) is one of two alternative sigma factors in *R. sphaeroides* besides $RpoH_I$ (σ^{37}), which are described as heat shock sigma factors. The two paralogs share 46% amino acid identity, and each sigma factor is able to complement a heat-sensitive *rpoH* deletion strain of *Escherichia coli* (12).

By proteome analysis of an *rpoH*$_{II}$ deletion strain, we showed that many of the RpoE-dependent proteins directly depend on $RpoH_{II}$ (22). Nevertheless, the synthesis of several proteins was reduced but not absent in the *rpoH*$_{II}$ deletion strain, and many other $^1O_2$-triggered proteins do not even contain a putative $RpoH_{II}$-specific promoter sequence. Therefore, other factors which lead to the induction of these genes by $^1O_2$ exposure must exist. The earlier findings that the relative expression of *rpoH*$_I$ is also strongly induced under $^1O_2$ stress (22) and that the *hslO* gene carries a heat-inducible promoter recognized by $RpoH_I$ and $RpoH_{II}$ (12) motivated us to analyze the role of $RpoH_I$ in the photooxidative stress response of *R. sphaeroides*.

For this purpose we constructed and characterized an *rpoH*$_I$ single-deletion strain and an *rpoH*$_I$ *rpoH*$_{II}$ double-deletion strain. We tested the sensitivity of these mutants to $^1O_2$, methylglyoxal, and increased/decreased temperatures. Moreover, the 5′ ends of selected $RpoH_{II}$ and $RpoH_I$/$RpoH_{II}$-dependent transcripts were mapped by rapid amplification of 5′ cDNA ends (5′-RACE) to get more detailed information about the promoter specificity of these sigma factors. Based on those data, we performed a genome-wide search for putative $RpoH_{II}$ and $RpoH_I$/$RpoH_{II}$ promoter sequences in close distance to open reading frames. In addition, we lately identified a set of small RNAs using high-throughput pyrosequencing (4). Here we demonstrate that expression of some small RNAs (sRNAs) is strongly dependent on $RpoH_I$ and $RpoH_{II}$.

MATERIALS AND METHODS

Bacterial strains and growth conditions. *R. sphaeroides* strains were grown at 32°C in minimal salt medium containing malate as the carbon source (9). Aerobic growth conditions with a concentration of 160 to 180 μM dissolved oxygen were established by gassing cultures with air in flat glass bottles or by continuous shaking of Erlenmeyer flasks at 140 rpm with a culture volume of 20%. In semiaerobic cultures, a volume of 80% in Erlenmeyer flasks and shaking at 140 rpm lead to a dissolved oxygen concentration of approximately 25 μM. When necessary, kanamycin (25 μg ml^{-1}), spectinomycin (10 μg ml^{-1}), tetracycline (1.5 μg ml^{-1}), or trimethoprim (50 μg ml^{-1}) was added to liquid and solid growth media, which contained 1.6% agar. Antibiotics were omitted from precultures, cultures, and agar plates used for *R. sphaeroides* strains during stress experiments and inhibition zone assays (see below) to ensure identical culture conditions. *Escherichia coli* strains were grown at 37°C in LB medium under continuous shaking at 180 rpm or on solid growth media.

* Corresponding author. Mailing address: Institut für Mikrobiologie und Molekularbiologie, Heinrich-Buff-Ring 26, 35392 Giessen, Germany. Phone: (49) 641 99 355 57. Fax: (49) 641 99 355 49. E-mail: Jens.Glaeser@mikro.bio.uni-giessen.de.

† Supplemental material for this article may be found at http://jb.asm.org/.

▽ Published ahead of print on 19 March 2010.

TABLE 1. Strains and plasmids

Strain/plasmid	Description	Source/reference
Strains		
E. coli		
S17-1	*recA pro hsdR* RP4-2-Tc::MuKm::Tn*7* *tra*$^+$ Km^r Sp^r	27
JM109	*recA1 supE44 endA1 hsdR17 gyrA96 relA1 thi (lac-proAB)*	New England Biolabs
R. sphaeroides		
2.4.1	Wild type	33
2.4.1(pRK415)	Wild type harboring pRK415, Tc^r	This study
TF18	*rpoE chrR* mutation in 2.4.1, Tp^r	26
TF18(pRK2.4.1*rpoEchrR*)	TF18 harboring pRK2.4.1*rpoEchrR*	This study
TF18(pRK415)	TF18 harboring pRK415, Tc^r	This study
2.4.1Δ*rpoH$_{II}$*	2.4.1*rpoH$_{II}$*::ΩSp^r/Sm^r	22
2.4.1Δ*rpoH$_{II}$*(pRK415)	2.4.1Δ*rpoH$_{II}$* harboring pRK415, Tc^r	26
2.4.1Δ*rpoH$_{II}$*(pRK2.4.1*rpoH$_{II}$*)	2.4.1Δ*rpoH$_I$* harboring pRK2.4.1*rpoH$_{II}$*	26
2.4.1Δ*rpoH$_I$*	2.4.1*rpoH$_I$*::Km^r cassette	This study
2.4.1Δ*rpoH$_I$*(pRK415)	2.4.1Δ*rpoH$_I$* harboring pRK415, Tc^r	This study
2.4.1Δ*rpoH$_I$*(pRK2.4.1*rpoH$_I$*)	2.4.1Δ*rpoH$_I$* harboring pRK2.4.1*rpoH$_I$*	This study
2.4.1Δ*rpoH$_I$* Δ*rpoH$_{II}$*	2.4.1Δ*rpoH$_{II}$ rpoH$_I$*::Km^r cassette	This study
2.4.1Δ*rpoH$_I$* Δ*rpoH$_{II}$*(pRK415)	2.4.1Δ*rpoH$_I$* Δ*rpoH$_{II}$* harboring pRK415, Tc^r	This study
2.4.1Δ*rpoH$_I$* Δ*rpoH$_{II}$* (pRK2.4.1*rpoH$_I$*)	2.4.1Δ*rpoH$_I$* Δ*rpoH$_{II}$* harboring pRK2.4.1*rpoH$_I$*	This study
TF18Δ*rpoH$_I$*	TF18 *rpoH$_I$*::Km^r cassette	This study
TF18Δ*rpoH$_I$*(pRK415)	TF18Δ*rpoH$_I$* harboring pRK415, Tc^r	This study
TF18Δ*rpoH$_I$*(pRK2.4.1*rpoH$_I$*)	TF18Δ*rpoH$_I$* harboring pRK2.4.1*rpoH$_I$*	This study
Plasmids		
pPHU281	Suicide vector for *R. sphaeroides*, Tc^r	15
pUC4K	Km^r, source of Km^r cassette	25
pRK415	Tc^r	18
pPHU2.4.1*rpoH$_I$*::Km^r	pPHU281 with Km^r cassette, flanked by the upstream and downstream regions of *rpoH$_I$*	This study
pRK2.4.1*rpoH$_I$*	pRK415 harboring a 1.2-kb fragment containing *rpoH$_I$*, flanked by the 239-bp upstream and 26-bp downstream regions	This study
pRK2.4.1*rpoEchrR*	pRK415 harboring a 1.6-kb fragment containing the *rpoE-chrR* operon, flanked by the 241-bp upstream and 158-bp downstream regions	This study
pDrive cloning vector	Ap^r Km^r	Qiagen

Construction of *R. sphaeroides rpoH$_I$* deletion strains. *R. sphaeroides* strains 2.4.1Δ*rpoH$_I$*, 2.4.1Δ*rpoH$_I$* Δ*rpoH$_{II}$*, and 2.4.1TF18Δ*rpoH$_I$* were generated by transferring the suicide plasmid pPHU2.4.1*rpoH$_I$*::Km (Table 1) into *R. sphaeroides* 2.4.1, 2.4.1Δ*rpoH$_{II}$*, and the *rpoE chrR* mutant strain TF18. Knockout candidates were screened for insertion of the kanamycin cassette into the chromosome by homologous recombination. Parts of the *rpoH$_I$* gene of *R. sphaeroides* 2.4.1 together with upstream and downstream sequences were amplified by PCR using the oligonucleotides 2.4.1*rpoH$_I$*_knockout-up_EcoRI, 2.4.1*rpoH$_I$*_knockout-up_BamHI, 2.4.1*rpoH$_I$*_knockout-down_BamHI, and 2.4.1*rpoH$_I$*_knockout-down_SphI (see Table S1 in the supplemental material). The obtained PCR fragments were cloned into pPHU281 (15), using the appropriate restriction endonucleases. Then, the kanamycin cassette obtained from the plasmid pUC4K (34) was inserted into the BamHI restriction site to obtain the plasmid pPHU2.4.1*rpoH$_I$*::Km. The plasmid pPHU2.4.1*rpoH$_I$*::Km was transferred into *E. coli* strain S17-1 (27) and mobilized into *R. sphaeroides* strains by biparental conjugation. Conjugants were selected on malate minimal medium agar plates containing 25 μg kanamycin ml^{-1}.

PCR analysis of chromosomal DNA isolated from kanamycin-resistant and tetracycline-sensitive conjugants was carried out to confirm the double-crossover event of the kanamycin cassette into the *R. sphaeroides* chromosome. For this purpose, the whole *rpoH$_I$* gene, including 6 bp of the upstream region and 365 bp of the downstream region, was PCR amplified using primers 2.4.1*rpoH$_I$*-test-A and 2.4.1*rpoH$_I$*-test-B (see Table S1 in the supplemental material). By insertion of the kanamycin cassette, 676 bp of the 897-bp *R. sphaeroides rpoH$_I$* gene were deleted. For the double-crossover candidates, only one PCR fragment, with a size of 1,885 bp, consisting of the flanking regions of the *rpoH$_I$* gene (592 bp) and the 1,293-bp kanamycin cassette, was obtained. For single-crossover candidates, the following two PCR fragments were obtained: a smaller fragment with the entire *rpoH$_I$* gene, including the flanking regions (1,268 bp), which was also observed for the wild type, and a larger fragment with the deleted *rpoH$_I$* gene, including the kanamycin cassette (1,885 bp).

Complementation of the *R. sphaeroides rpoH$_I$* and *rpoE* deletion strains. For complementation of *rpoH$_I$* deletion strains, a 1,162-bp PCR fragment containing the entire *rpoH$_I$* gene along with 239 bp of the upstream sequence and 26 bp of the downstream sequence was amplified using the oligonucleotides 2.4.1*rpoH$_I$*-upstream and 2.4.1*rpoH$_I$*-downstream (see Table S1 in the supplemental material). The obtained PCR fragment was cloned into the pDrive vector (Qiagen, Hilden, Germany). Digestion of the pDrive vector containing the insert with PstI and XbaI, followed by cloning with the same restriction sites into plasmid pRK415, obtained plasmid pRK2.4.1*rpoH$_I$*. This plasmid was subsequently transformed in *E. coli* S17-1 and conjugated with strain 2.4.1Δ*rpoH$_I$*, 2.4.1Δ*rpoH$_I$* Δ*rpoH$_{II}$*, and TF18Δ*rpoH$_I$* to obtain the complemented strains 2.4.1Δ*rpoH$_I$*(pRK2.4.1*rpoH$_I$*), 2.4.1Δ*rpoH$_I$* Δ*rpoH$_{II}$*(pRK2.4.1*rpoH$_I$*), and TF18Δ*rpoH$_I$* (pRK2.4.1*rpoH$_I$*).

For complementation of the *rpoE chrR* deletion strain TF18, a 1,595-bp PCR fragment containing the entire *rpoE-chrR* operon, along with 241 bp of the upstream sequence and 158 bp of the downstream sequence, was amplified using the oligonucleotides 2.4.1*rpoEchrR*-upstream and 2.4.1*rpoEchrR*-downstream (see Table S1 in the supplemental material). The obtained PCR fragment was cloned into the pDrive vector (Qiagen, Hilden, Germany). Digestion of the pDrive vector containing the insert with EcoRI, followed by cloning with the same restriction site into plasmid pRK415, obtained the plasmid pRK2.4.1*rpoEchrR*. This plasmid was subsequently transformed in *E. coli* S17-1 and conjugated with strain TF18 to obtain the complemented strain TF18(pRK2.4.1*rpoEchrR*).

Sensitivity to $^1O_2$, methylglyoxal, and changes in temperature. Measurement of sensitivity to $^1O_2$ and methylglyoxal was performed as described previously (22). Exponential-phase cultures grown under semiaerobic conditions at 32°C were used to test the effect of temperature changes on *R. sphaeroides* 2.4.1 and

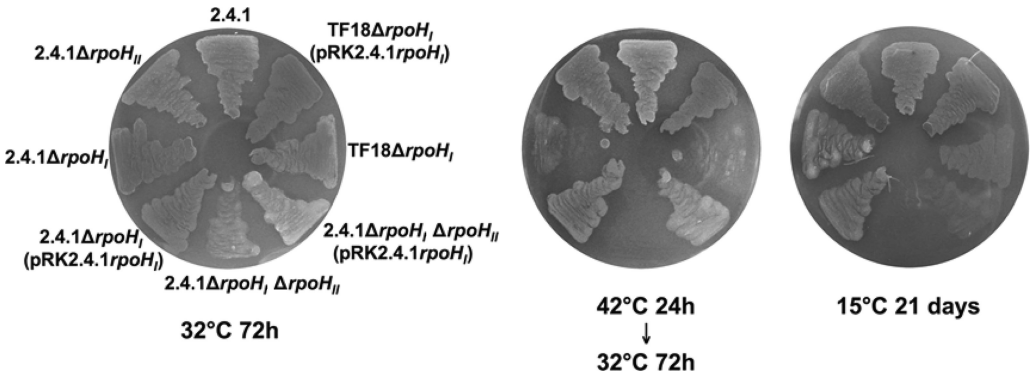

FIG. 1. Growth of *R. sphaeroides* wild-type and $rpoH_I$ and $rpoH_{II}$ deletion strains under different temperatures. The cultures were grown under semiaerobic conditions at 32°C to exponential phase and diluted to an OD_{660} of 0.1. For each strain, 5 μl of diluted culture was plated on minimal agar plates and incubated under the indicated temperatures in the dark. The agar plates incubated at 42°C were shifted to 32°C (optimal growth) after 24 h.

the $rpoH_I$ and $rpoH_{II}$ deletion strains (Table 1). Cultures were diluted to an optical density at 660 nm (OD_{660}) of 0.1, and for each strain, 5 μl of diluted culture was plated on agar plates, followed by incubation in the dark. Sensitivity to elevated temperatures was tested by incubating agar plates for 24 h at 42°C, followed by incubation at 32°C for 3 days to monitor growth. Growth was monitored also at 15°C for 21 days, and control agar plates were incubated at 32°C for 3 days.

High-light and photooxidative stress conditions. High-light and photooxidative stress conditions were performed as described earlier (10). In brief, cultures were grown under semiaerobic conditions overnight to obtain pigmented cells. Cultures were diluted to an OD_{660} of 0.2 and allowed to double once under aerobic growth conditions in darkened flat glass bottles. High-light conditions were generated by illumination with 800 W m^{-2} white light. For photooxidative stress, $^1O_2$-producing methylene blue was added to liquid cultures at a final concentration of 0.2 μM prior to illumination. Because these conditions are lethal for the $rpoH_I$ $rpoH_{II}$ double-deletion strain, illumination with 700 W m^{-2} and 0.2 μM methylene blue were used.

Radioactive labeling of proteins and gel-based proteome analysis. Radioactive labeling and proteome analysis performed by two-dimensional (2D) gel electrophoresis followed the procedure described earlier (11). In brief, samples of 7 ml were retrieved from *R. sphaeroides* cultures, 15 μCi L-[^{35}S]methionine (GE Healthcare, München, Germany) was added, and incubation was performed for 10 min under the experimental conditions described above. Samples were cooled on ice after incubation, and cells were harvested by centrifugation at 10,000 × *g* for 10 min at 4°C and stored at −20°C until further processing. For the extraction of soluble proteins, harvested cells were washed and disrupted by sonication. Intact cells and cell debris were removed by centrifugation, and the supernatant was used for ultracentrifugation at 100,000 × *g*. The radioactive label was quantified in the colorless supernatant by adding 10-μl aliquots to 1 ml Rotiszint scintillation cocktail (Roth, Karlsruhe, Germany) and measured in a Beckmann LS-6500 scintillation counter (Beckmann Coulter, Fullerton, CA). For 2D gel electrophoresis, protein samples containing 1.5 × 10^6 cpm were treated with RNase A (Qiagen) and RQ1 DNase I (Promega, Madison, WI) to remove nucleic acids. Proteins were precipitated using a final concentration of 10% trichloroacetic acid, and the protein pellets were dried and then solubilized in sample buffer (11). Then, samples were applied to immobilized pH gradient strips (ReadyStrip; Bio-Rad, Hercules, CA). After isoelectric focusing, proteins were separated by sodium dodecyl sulfate-polyacrylamide gel electrophoresis, and gels were fixed, dehydrated, dried, and exposed to phosphorimaging screens for 48 h. Phosphorimages were read with a Molecular Imager FX (Bio-Rad) set to a resolution of 100 μm. Protein spots on digital phosphorimages were compared using the software Delta2D version 3.3 (Decodon, Greifswald, Germany).

RNA extraction, 5′-RACE, and Northern blot analysis. RNA extraction for 5′-RACE and the 5′-RACE protocol was performed as described previously (22). For Northern blot analysis, samples from stress experiments were collected before (0 min) and 10 min after the onset of stress conditions. From these samples, total RNA was isolated by the hot phenol method (16) and quantified photometrically using a wavelength of 260 nm. Total RNA was separated on 10% polyacrylamide gels containing 7 M urea and then transferred onto Biodyne B 0.45-μm membranes (Pall) by semidry electroblotting. A total of 10 to 20 μg RNA per sample was loaded. Detection of the sRNAs RSs0680a and RSs2461 was carried out as described earlier (4). For detection of the newly identified sRNA RSs1543, the end-labeled oligodeoxynucleotide p-1543 (5′-ATG AAG CGG ACG AGA GAA CCC TC-3′) was used. Membranes were exposed on phosphorimaging screens (Bio-Rad) and analyzed with the Quantity One 1-D software (Bio-Rad).

Real-time RT-PCR. The primers employed for analyzing relative expression of target genes using real-time reverse transcription-PCR (RT-PCR) are listed in Table S1 in the supplemental material. For normalization of mRNA levels, the *rpoZ* gene, which encodes the ω subunit of RNA polymerase of *R. sphaeroides*, was used (23). Conditions for real-time RT-PCR were described earlier in detail (10, 11). For real-time RT-PCR, a final concentration of 4 ng μl^{-1} of total RNA was applied in a one-step RT-PCR kit (Qiagen), and SYBR green I (Sigma-Aldrich) was added in a final dilution of 1:50,000 to the master mix to detect double-stranded DNA. Relative expression of target genes was calculated relative to expression of untreated samples and relative to *rpoZ* (24). PCR efficiency is 2.02 for *rpoZ* (10, 11), and further PCR efficiencies were determined experimentally using serial dilutions of RNA; respective values obtained are 2.12 for *qxtA*, 2.07 for RSP0150, 2.19 for RSP1948, and 1.9 for *hslO*.

Genome-wide prediction of sigma factor target sites. Based on the information on transcriptional start sites gained by 5′-RACE, putative sigma factor binding sites were identified. We then used those binding sites to create consensus sequences for promoters recognized only by $RpoH_{II}$ or by $RpoH_I$ and $RpoH_{II}$. For a genome-wide prediction of putative sigma factor binding sites, those consensus sequences were used to search the *R. sphaeroides* 2.4.1 genome by using the DNA genome-scale DNA pattern software within the regulatory sequence analysis (RSA) tools (http://rsat.ulb.ac.be/rsat) (32). The whole chromosome was searched, and putative promoter positions were then analyzed with respect to their locations in intergenic regions or upstream of mRNA coding regions using ARTEMIS 11 software. Transcriptional start sites obtained previously by pyrosequencing of $^1O_2$ and superoxide-treated *R. sphaeroides* cultures (4) were used to verify putative promoters obtained by the bioinformatic prediction.

Statistical analysis. Statistical analysis for the comparison of threshold cycle values obtained for individual genes under different stress conditions using real-time RT-PCR was performed with Student's *t* test using Microsoft Excel 2003 (Microsoft, Redmond, WA). Significance levels (*P* of ≤0.1, ≤0.05, and ≤0.01) are indicated in the figure legends.

RESULTS

Deletion of $rpoH_I$ and $rpoH_{II}$ differently affects sensitivity to temperature, $^1O_2$, and methylglyoxal. The construction of $rpoH_I$ deletion strains in the *R. sphaeroides* 2.4.1, 2.4.1$rpoH_{II}$, and *rpoE chrR* mutant strain TF18 backgrounds yielded the strains 2.4.1Δ$rpoH_I$, 2.4.1Δ$rpoH_I$ Δ$rpoH_{II}$, and TF18Δ$rpoH_I$ as described in Materials and Methods. We tested the sensitivity of the *rpoH* deletion strains to changes in temperature (Fig. 1), $^1O_2$, and methylglyoxal (Fig. 2). The $rpoH_I$ $rpoH_{II}$ deletion

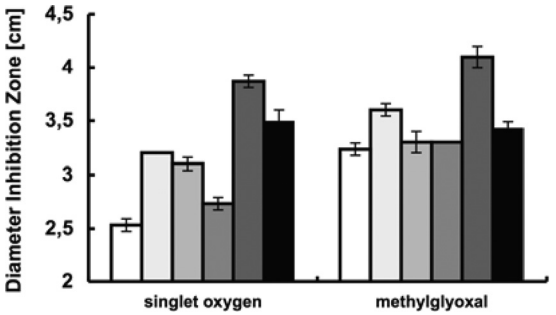

FIG. 2. Inhibition of growth of the *R. sphaeroides* wild type, the TF18 strain, and the *rpoH*$_I$ and *rpoH*$_{II}$ deletion strains by $^1O_2$ and methylglyoxal. Each point represents the mean result from three independent experiments. Error bars indicate the maximal deviations from three experiments. 2.4.1, open; 2.4.1Δ*rpoH*$_{II}$, light gray (second bar); TF18(*rpoE chrR* mutant), gray (third bar); 2.4.1Δ*rpoH*$_I$, dark gray (fourth bar); 2.4.1Δ*rpoH*$_I$ Δ*rpoH*$_{II}$, dark gray (fifth bar); and TF18(*rpoE chrR* mutant)Δ*rpoH*$_I$, filled.

strain was most sensitive to all three stress factors compared to the other mutants and the wild-type strain. It was not growing on agar plates incubated at 15°C as well as after 24 h of incubation at 42°C. Inhibition zones obtained for $^1O_2$ and methylglyoxal treatment were larger than those in all other strains tested (Fig. 2). Deletion of the *rpoH*$_I$ gene in strain TF18 was performed to test if dependency of *rpoH*$_{II}$ expression on RpoE leads to a phenotype similar to that of the *rpoH*$_I$ *rpoH*$_{II}$ deletion strain. Strain TF18Δ*rpoH*$_I$ exhibited a less sensitive phenotype for all three stress factors compared to that of the *rpoH*$_I$ *rpoH*$_{II}$ deletion strain but was more affected by $^1O_2$ exposure than the parent strain TF18 (Fig. 2). Strain TF18 was not affected by changes in temperature, similar to the complemented *rpoH*$_I$ deletion strain TF18Δ*rpoH*$_I$ (Fig. 1). The less pronounced sensitivity of strain TF18Δ*rpoH*$_I$ compared to that of the *rpoH*$_I$ *rpoH*$_{II}$ deletion strain is in agreement with the finding that *rpoH*$_{II}$ expression is not entirely dependent on RpoE (22). The deletion of *rpoH*$_I$ in the wild-type and TF18 background generated a phenotype sensitive to increased temperature but not to decreased temperature (Fig. 1). In comparison, deletion of *rpoH*$_{II}$ in the wild type generated a phenotype more sensitive to $^1O_2$ and methylglyoxal but not to temperature changes (22) (Fig. 1 and 2). Complementation with low-copy-number plasmid pRK415 harboring the *rpoH*$_I$ gene with its own promoter region restored the phenotype of the respective parental strains (Fig. 1; see also Table S2 in the supplemental material), except for strain 2.4.1Δ*rpoH*$_I$ Δ*rpoH*$_{II}$(pRK2.4.1*rpoH*$_I$) which showed weaker growth at 15°C compared to strain 2.4.1Δ*rpoH*$_{II}$ (Fig. 1). The presence of the plasmid pRK415 without the *rpoH*$_I$ gene did not influence the sensitivity of the strains to $^1O_2$ and methylglyoxal (see Table S2) or to increased and decreased temperatures (data not shown).

Proteome analysis reveals overlapping RpoH$_I$ and RpoH$_{II}$ regulons. In a recent study we found that 25 soluble proteins induced by $^1O_2$ exposure were strongly affected by the deletion of *rpoH*$_{II}$ (22). The majority of those proteins were not synthesized in the *rpoH*$_{II}$ deletion strain, but several proteins were decreased only in synthesis. *In vitro* studies suggested that RpoH$_I$ and RpoH$_{II}$ of *R. sphaeroides* 2.4.1 recognize the same

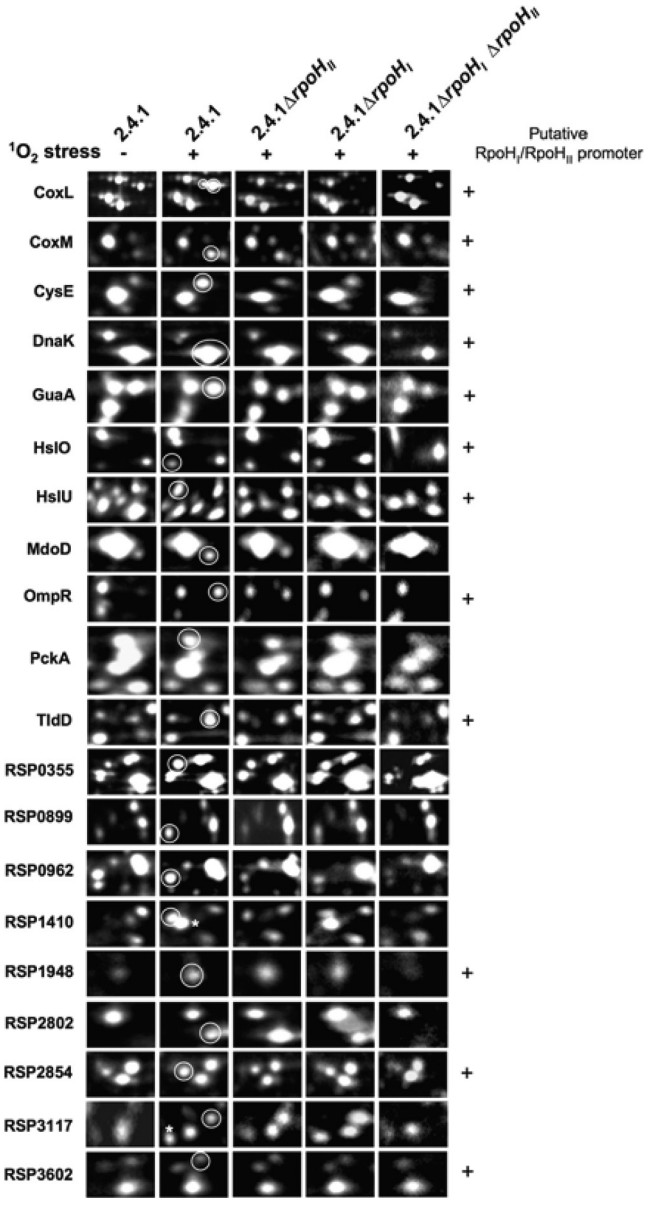

FIG. 3. Sections of inverted 2D gel images indicating differences in syntheses of several proteins between the wild-type strain 2.4.1 and strains 2.4.1Δ*rpoH*$_{II}$, 2.4.1Δ*rpoH*$_I$, and 2.4.1Δ*rpoH*$_I$ Δ*rpoH*$_{II}$ after 60 min of $^1O_2$ exposure. Protein extracts were prepared from cells labeled *in vivo* with L-[^{35}S]methionine during exponential growth in the dark or in the presence of methylene blue and high light. Proteins labeled with RSP numbers have hypothetical function, and those marked with asterisks were shown previously to be dependent on RpoH$_{II}$ (22).

set of heat-inducible promoters (12). Consequently, we assessed the role of potentially overlapping RpoH$_I$ and RpoH$_{II}$ regulons in the cellular defense against excess $^1O_2$ generation. Patterns of soluble proteins obtained from the *rpoH*$_I$ and the *rpoH*$_I$ *rpoH*$_{II}$ deletion strains were compared with those obtained from the wild-type strain 2.4.1 and the *rpoH*$_{II}$ deletion strain (Fig. 3; see also Fig. S1 and S2 in the supplemental material) and revealed that RpoH$_I$ and RpoH$_{II}$ regulons indeed partially overlap.

In our previous study, some proteins were induced in the

rpoH$_{II}$ deletion strain by $^1O_2$ exposure but to a lower level than in the wild type (22). We observed that several proteins were fully synthesized upon $^1O_2$ exposure in the wild-type strain and to the same or to a lower level in the *rpoH*$_I$ and *rpoH*$_{II}$ deletion strains, but those proteins were lacking in the *rpoH*$_I$ *rpoH*$_{II}$ deletion strain (Fig. 3). This observation was made for the protein CysE (serine *O*-acetyltransferase), which showed a decreased synthesis in the *rpoH*$_{II}$ deletion strain compared to that of the wild type (22) and was not synthesized in the *rpoH*$_I$ *rpoH*$_{II}$ deletion strain (Fig. 3). In a similar manner, CoxL (RSP2877, xanthine dehydrogenase, molybdenum binding subunit apoprotein), CoxM (RSP2876, putative carbon monoxide dehydrogenase, medium chain), HslO (putative Hsp33 protein), HslU (RSP1532, ATP-dependent protease ATP-binding subunit), MdoD (RSP3187, glucan biosynthesis protein D), OmpR (RSP0847, two-component transcriptional regulator), TldD (RSP1825, modulator of DNA gyrase), RSP0355 (serine protease), RSP0899 (thiol peroxidase [atypical 2-Cys peroxiredoxin]), RSP1410 (putative sulfite oxidase subunit), RSP1948 (hypothetical protein), RSP2802 (multidrug/cation efflux pump, membrane fusion protein subunit), RSP2854 (cation efflux transporter), and RSP3117 (hypothetical protein) were either not synthesized upon $^1O_2$ exposure in the *rpoH*$_I$ *rpoH*$_{II}$ deletion strain or induction was lacking and the respective protein was synthesized in an amount similar to that in the nonexposed wild type (Fig. 3) and the *rpoH* single deletion strain (data not shown). The synthesis of the proteins DnaK (RSP1173, molecular chaperone), GuaA (RSP0005, GMP synthase), PckA (RSP1680, phosphoenolpyruvate carboxykinase), RSP0962 (dihydrolipoamide dehydrogenase), and RSP3602 (ABC efflux transporter, ATPase subunit) was not induced by $^1O_2$ stress. These proteins were not synthesized or synthesized at lower levels in the *rpoH*$_I$ *rpoH*$_{II}$ deletion strain than in the wild type and the *rpoH*$_I$ and *rpoH*$_{II}$ deletion strains. This finding suggests a role of those proteins in basic cellular physiology and implies that they are not specific for the defense to stress generated by $^1O_2$ exposure. Interestingly, HslU was the only protein observed in this study that was not synthesized in the *rpoH*$_I$ deletion strain and therefore seems to depend only on $RpoH_I$ under photooxidative stress.

Target sequences recognized by $RpoH_{II}$ and $RpoH_I/RpoH_{II}$. Our proteome data demonstrate that the synthesis of several proteins depends on both $RpoH_I$ and $RpoH_{II}$. In order to identify sigma factor binding sites recognized by $RpoH_I$ and $RpoH_{II}$, we analyzed the upstream region of the genes encoding OmpR and RSP1948 by 5′-RACE (Fig. 4). For both genes, putative sigma factor binding sites similar to the heat-inducible promoters upstream of *rpoD* and *ecfE* (12) were observed upstream of the determined 5′ ends. Both binding sites differ from those supposed to be recognized only by $RpoH_{II}$ (22). To find differences between $RpoH_{II}$- and $RpoH_I/RpoH_{II}$-specific promoters, we also mapped the 5′ ends of further mRNA transcripts strictly depending on $RpoH_{II}$, including RSP0423, RSP0663, RSP2268, and RSP3164.

For all six selected mRNAs, we monitored relative changes in the intensity of 5′-RACE-PCR products obtained in *R. sphaeroides* 2.4.1, the *rpoH*$_{II}$, the *rpoH*$_I$, and the *rpoH*$_I$ *rpoH*$_{II}$ deletion strains (Fig. 4A). For *rpoZ*, which served as an internal control (36), PCR products from all strains were highly similar in intensity, which indicates that global transcript levels

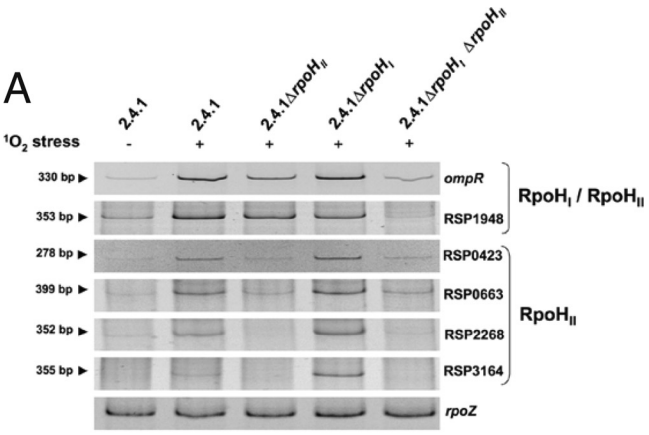

B

$RpoH_I/RpoH_{II}$

	-35	-10 region
‡*dnaK*	cgc**TTG**c..N_{18}..**CTATAT**acgcccggt-N_{106}	**-atg**
‡*cycA* P1	gta**GTG**a..N_{17}..**CTATAT**ctttaccac-N_{26}	**-atg**
‡*hslO*	ccc**TTG**g..N_{17}..**CTATAT**tggggcggt-N_{30}	**-atg**
‡*rpoD* P_{HS}	ccc**TTG**a..N_{18}..**CCATGT**tcgcatctg-N_{402}	**-atg**
ompR	atc**TTG**c..N_{18}..**ACATGT**gatcggca -N_{18}	**-atg**
RSP1948	gac**TTG**a..N_{18}..**CCATAT**ccctcgga -N_{19}	**-atg**
‡*ecfE*	ccc**TTG**a..N_{18}..**CCATCT**cgctcggag-N_{49}	**-ttg**
consensus	**KTG** N_{18-19}	**MYATVT**

$RpoH_{II}$

**gloA*	ccg**TTT**c..N_{17}..**CTAGCT**tgcgcgcca-N_{20}	**-atg**
**gst*	ccc**TTG**c..N_{16}..**CTAGCT**ctgggagg -N_{10}	**-atg**
*RSP3075	gcg**GTG**g..N_{18}..**CTAGCT**ggaggctc -N_{19}	**-atg**
RSP2268	cca**TTT**c..N_{17}..**CTAGAT**tgcagccga-N_{27}	**-atg**
RSP0663	ggc**TCG**a..N_{18}..**CTAGAT**ccgtcgtg -N_{34}	**-atg**
RSP3164	ctc**TTG**a..N_{17}..**CTAGGT**ggccgccaa-N_{18}	**-atg**
consensus 1	**KBB** N_{17-19}	**CTAGVT**
RSP0150	cca**TTG**g..N_{17}..**CTAGGCT**gttgcga-N_{26}	**-ttg**
RSP0423	gcc**TTG**c..N_{17}..**CTAGGCT**gcaaccgc-N_{16}	**-atg**
consensus 2	**KBB** N_{18}	**CTAGSST**

K: T or G
Y: T or C
B: C, T or G
V: A, C or G
M: C or A

FIG. 4. (A) Separation of 5′-RACE products obtained from RNA extracts of wild-type and *rpoH*$_I$ and *rpoH*$_{II}$ deletion strains after 10 min of photooxidative stress. PCR products obtained after the second PCR (nested) were separated on a 10% polyacrylamide gel and stained with ethidium bromide. (B) Upstream of the 5′ ends of the sequences corresponding to the depicted DNA bands, putative $RpoH_{II}$ target sequences were found and displayed as an alignment. 5′ ends are underlined. ‡, $RpoH_I/RpoH_{II}$-dependent promoters verified by *in vitro* transcription (12); boldfaced letters, putative target sequences identified in this study; ∗, putative target sequences identified earlier (22). To match relative changes in mRNA levels of the respective genes, cDNA synthesis with all gene-specific RACE-1 primers in the same reaction was performed (see Table S1 in the supplemental material). We used a primer specific for *rpoZ*, a gene used for normalization in the real-time RT-PCR approach described earlier (23).

are not affected in the respective deletion strains or by $^1O_2$ treatment. For all six other mRNAs, PCR products were amplified from wild-type cultures exposed to $^1O_2$. The products were less abundant or missing using RNA extracts of the un-

stressed wild type compared to using the $^1O_2$ stressed wild type. 5′-RACE for *ompR* and RSP1948 further supported the results obtained from proteome analysis. Expression of both genes depends on $RpoH_I$ and $RpoH_{II}$, since strong PCR products were observed in all strains except for the *rpoH$_I$ rpoH$_{II}$* deletion strain. PCR products were much weaker for *ompR* in the double-deletion strain than in all other strains exposed to $^1O_2$, and products were lacking for RSP1948 (Fig. 4A). For RSP0423, RSP0663, RSP2268, and RSP3164, amplification of PCR products obtained from RNA extracts of the *rpoH$_{II}$* and *rpoH$_I$ rpoH$_{II}$* deletion strains were much weaker or missing in comparison to those of the wild type and the *rpoH$_I$* deletion strain (Fig. 4A), underlining the strong dependence on only $RpoH_{II}$ (22).

We identified putative sigma factor target sequences directly upstream of the 5′ ends of all tested genes (Fig. 4B). The putative sigma factor target sequences identified upstream of the $RpoH_{II}$-dependent genes RSP0423, RSP0663, RSP2268, and RSP3164 were highly similar to those identified earlier (22). By combining the information gained on the sigma factor target sequences, we identified a conserved consensus motif consisting of CTAGVT (V: A, C, or G) in the −10 region of $RpoH_{II}$-dependent target sequences. Interestingly, the −10 region of the sigma factor target sequence upstream of RSP0423 exhibited an additional base pair in the hexameric motif CTAGVT, forming the heptameric −10 region CTAG GCT. In contrast, the −10 region also recognized by $RpoH_I$ consists of an MYATVT (M, C or A; Y, T or C) consensus motif. This motif shows high similarity to the RpoH-dependent promoter described for *Caulobacter crescentus* (TNNCNCCC **TTG**AA-$N_{13–15}$-CC**CCATNT**A) (35) and to the *E. coli* RpoH promoter consensus sequence (CNC**TTG**AAA-$N_{13–14}$-CC**CCATNT**) (13) (boldface shows similarities).

Genome-wide search for $RpoH_{II}$ and $RpoH_I$/$RpoH_{II}$ target sequences. In order to predict promoters exhibiting $RpoH_{II}$ or $RpoH_I$/$RpoH_{II}$ target sites and thereby the respective regulons, we used the genome-scale DNA pattern software within the RSA tools (32). We used the −10 region consensus sequences recognized by $RpoH_{II}$ (Fig. 4B) and the respective consensus of the −35 region. Precisely, the *R. sphaeroides* 2.4.1 genome was searched for putative $RpoH_{II}$-dependent promoters with the motif KBB-$N_{17–19}$-CTAGVT (K: T or G; B: T, C, or G; V: A, C, or G), which revealed 47 highly conserved target sites not more than 400 bp upstream of translational start sites of protein coding genes (Table 2). Additionally, we searched for the motif KBB-$N_{17–19}$-CTAGSST and identified 68 genes preceded by a putative $RpoH_{II}$ promoter with a heptameric −10 region (see Table S3 in the supplemental material). In a third search, the motif KTG-$N_{(18–19)}$-MYATVT was used to identify putative $RpoH_I$/$RpoH_{II}$-dependent promoters, which gained 170 putative target genes (see Table S4 in the supplemental material). In all searches, we included only those target sites exhibiting at least one "T" in the −35 element.

The genome-wide location of putative $RpoH_{II}$ and $RpoH_I$/$RpoH_{II}$ target sites was verified by comparison to that of primary transcripts obtained by 454 pyrosequencing that were aligned to the *R. sphaeroides* 2.4.1 genome (4). For almost one-third of our predicted promoters, we identified a 5′ end of the respective mRNA 5 to 10 bp downstream of the −10 region (Table 2; see also Tables S3 and S4 in the supplemental material).

Among those genes preceded by an $RpoH_{II}$- or $RpoH_I$/$RpoH_{II}$-dependent promoter, several encode proteins typically involved in stress responses, but also proteins are encoded which are involved in basic cellular responses, e.g., energy metabolism, transport, protein turnover, and other functions like lipid metabolism. In our search for $RpoH_I$/$RpoH_{II}$-dependent promoters, we identified a number of genes encoding proteins known to be involved in the heat stress response, e.g., DnaK, GroES, GrpE, HslO, HrcA, HslV, HtpX, and IbpA (see Table S4 in the supplemental material).

Verification of $RpoH_{II}$-dependent gene expression. We tested the expression of three genes that were predicted to exhibit an $RpoH_{II}$-dependent promoter by real-time RT-PCR. We focused on *qxtA* (RSP3212), encoding the quinol oxidase subunit I, with a predicted hexameric −10 region in the $RpoH_{II}$ target sequence (Table 2). In addition, we analyzed the following two genes preceded by heptameric, potentially $RpoH_{II}$-specific −10 regions in the promoter sequence: RSP0150, a putative multi-sensor signal transduction histidine kinase related to bacteriophytochromes, and *cryB* (RSP3077), a bacterial cryptochrome (see Table S3 in the supplemental material) (16). After $^1O_2$ exposure, mRNA levels were increased up to 4-fold for RSP0150, more than 12-fold for *qxtA*, and ~3-fold for *cryB* in the wild type. For all three genes, mRNA levels did not increase in the *rpoH$_{II}$* and the *rpoH$_I$ rpoH$_{II}$* deletion strains, but fold changes in mRNA levels were increased in the *rpoH$_I$* deletion strain (Fig. 5), indicating strong dependency on $RpoH_{II}$. Mapping of the 5′ end of the RSP0150 mRNA then verified a putative promoter highly similar to the promoter upstream of RSP0423 (Fig. 4B). A similar promoter was also found to precede the *cryB* gene (see Table S3) (14).

$RpoH_I$/$RpoH_{II}$-dependent sRNAs are induced by $^1O_2$ and heat stress. In a genome-wide search for primary transcripts using a 454 pyrosequencing approach, four abundant sRNAs were affected by $^1O_2$ exposure (4). Two of these sRNAs, RSs0680a and RSs2461, were supposed to be transcribed from an $RpoH_I$/$RpoH_{II}$ promoter. The 454 pyrosequencing data revealed the presence of a third sRNA, RSs1543, with a length of 83 nucleotides (nt), that is triggered by photooxidative stress. RSs0680a and RSs2461 are cotranscribed with upstream genes and lack their own promoters (4). In detail, RSs0680a is cotranscribed with RSP6037 (hypothetical protein) from the putative promoter TTG-N_{19}-CCATGT-N_{75}-ATG. The sRNA RSs2461 is cotranscribed with the *ompR* gene and thereby transcribed from the promoter upstream of *ompR* (Fig. 4B; see also Table S4 in the supplemental material). In contrast, RSs1543 is directly preceded by a promoter (Fig. 6a) with high similarity to the putative $RpoH_I$/$RpoH_{II}$ consensus motif, consisting of TTG-N_{19}-CTAAAT. Northern blot analysis revealed that all three sRNAs depend on both $RpoH_I$ and $RpoH_{II}$. The two sRNAs, RSs0680a and RSs1543, were strongly induced after 10 min of $^1O_2$ exposure in the wild type and the *rpoH$_I$* and *rpoH$_{II}$* single-deletion strains but not in the *rpoH$_I$ rpoH$_{II}$* double-deletion strain (Fig. 6B). For the third sRNA, RSs2461, the result was similar, but the induction was less pronounced. We also tested if the three sRNAs are inducible under heat stress conditions (Fig. 6B). An induction was observed for all three sRNAs 10 min after the shift from 32°C to 42°C, which fits into

TABLE 2. Conserved $RpoH_{II}$ target sequences upstream of protein coding genes[a]

Target sequence	ATG distance (bp)	Locus tag	Annotated protein(s)	5′ end
Energy metabolism				
TGT-N_{17}-CTAGAT	33	RSP2785-2784	CycF, cytochrome 554	+
TTG-N_{17}-CTAGAT	35	RSP3212-3210	QxtA, quinol oxidase subunit I	
TCG-N_{19}-CTAGAT	82	RSP3831	Cox15, putative cytochrome oxidase assembly factor	
Transport				
TTG-N_{19}-CTAGAT	31	RSP0367	Preprotein translocase SecG subunit	
TGG-N_{19}-CTAGCT	40	RSP0759	Putative capsule polysaccharide exporter	+
TTG-N_{19}-CTAGGT	34	RSP1053	Signal recognition particle Ffh	
TGC-N_{18}-CTAGCT	−28	RSP1497	Putative outer membrane lipoprotein carrier protein	+
TTG-N_{19}-CTAGCT	8	RSP1803-1805	CcmC, ABC heme transporter	+
TTC-N_{19}-CTAGGT	−2	RSP1843	FtsY, signal recognition particle-docking protein	
TTG-N_{18}-CTAGCT	129	RSP1882-1886	ABC polyamine transporter, ATPase subunit	
Regulatory proteins				
TGG-N_{19}-CTAGGT	29	RSP0269	TspO, tryptophane-rich sensory protein	
TTG-N_{19}-CTAGGT	42	RSP0762-0761	Transcriptional regulator XRE family	
TGG-N_{19}-CTAGAT	83	RSP2165	PutR, transcriptional regulator, AsnC family	
TTT-N_{19}-CTAGCT	43	RSP3217	Cache sensor signal transduction histidine kinase	
TCG-N_{18}-CTAGCT	20	RSP3430-3431	Transcriptional regulator, winged helix family	
TTG-N_{19}-CTAGCT	8	RSP3865	Predicted transcriptional regulator	+
TTG-N_{19}-CTAGGT	133	RSP4257-4258	Anti-sigma factor antagonist STAS	+
Protein turnover and amino acid metabolism				
GTG-N_{19}-CTAGCT	49	RSP0398	GdhA, glutamate/leucine dehydrogenase	
TTT-N_{19}-CTAGAT	34	RSP2627	HisI, Phosphoribosyl-AMP cyclohydrolase	
TTT-N_{18}-CTAGGT	27	RSP4043-4042	Peptidylprolyl isomerase	+
TTG-N_{19}-CTAGAT	364	RSP4294	16S rRNA	
TTG-N_{19}-CTAGAT	65	RSP4330	tRNA-Ala-GGC	
TTG-N_{19}-CTAGAT	364	RSP4347	16S rRNA	+
TTG-N_{18}-CTAGCT	30	RSP6044	Serine/alanine racemase	
Stress response				
TTT-N_{19}-CTAGCT	29	RSP0392	GloA, probable lactothioglutathione synthetase	
TCG-N_{19}-CTAGAT	42	RSP0663	Formate-tetrahydrofolate ligase	
GTC-N_{19}-CTAGAT	−2	RSP0817-0816	Aminodeoxychorismate synthase	
TTG-N_{17}-CTAGCT	18	RSP1591	Predicted glutathione *S*-transferase	+
TGG-N_{19}-CTAGCT	21	RSP1869	2-octaprenyl-6-methoxyphenyl hydroxylase	+
TTT-N_{19}-CTAGAT	8	RSP2092	Putative *uvrD*/DNA helicase II	+
GGT-N_{18}-CTAGCT	202	RSP2123	Radical SAM domain protein and/or SplB, DNA repair photolyase domain	
TTG-N_{18}-CTAGAT	62	RSP2617	Peptide methionine sulfoxide reductase	+
TGT-N_{18}-CTAGGT	394	RSP2647-2648	Predicted SAM-dependent methyltransferase	+
TTG-N_{18}-CTAGGT	27	RSP3164-3162	Ferredoxin-like protein	+
TTG-N_{17}-CTAGAT	35	RSP3212-3210	QxtA, Quinol oxidase subunit I	
Hypothetical				
TTC-N_{19}-CTAGCT	29	RSP0238	Hypothetical protein	
TTC-N_{17}-CTAGCT	28	RSP0855	Hypothetical protein	+
TTG-N_{18}-CTAGCT	110	RSP1366	Hypothetical protein	
TGG-N_{19}-CTAGAT	30	RSP1421	Hypothetical protein	+
GTG-N_{19}-CTAGCT	27	RSP3075-3076	Hypothetical protein	+
TTG-N_{19}-CTAGCT	29	RSP6001	Hypothetical protein	+
TTC-N_{19}-CTAGCT	237	RSP6037	Hypothetical protein	
TTG-N_{19}-CTAGCT	31	RSP6232	Hypothetical protein	
Other functions				
GGT-N_{18}-CTAGAT	121	RSP1502	GAF domain protein	
TTT-N_{19}-CTAGGT	16	RSP1896	Guanine deaminase	
TTT-N_{18}-CTAGAT	36	RSP2268	Metallo-beta-lactamase family	
TCT-N_{19}-CTAGAT	70	RSP2468-2470	Putative portal protein	
TCG-N_{19}-CTAGAT	30	RSP3261-3262	BioA, aminotransferase	

[a] The target sequences listed were searched using the RSA tools and the consensus sequence KBB-N_{17-19}-CTAGVT. The distance to the translational start site is listed, and it is indicated if downstream genes might be cotranscribed and, hence, may form an operon. Negatives distances to the translational start sites indicate that the start codon might have been annotated incorrectly. Positives (+) in the "5′ end" column indicate that primary transcripts were found using 454 pyrosequencing (4) and that the respective sigma factor target sequence is located directly upstream of the 5′ end.

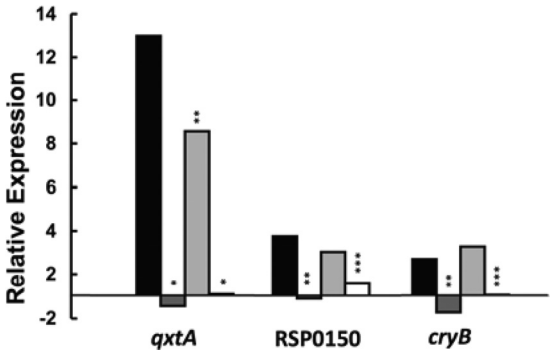

FIG. 5. Selected functional genes depending on $RpoH_{II}$ for expression, predicted by genome-wide search for putative $RpoH_{II}$ target sequences. Relative expression of *qxtA*, RSP0150, and *cryB* in strains 2.4.1 (black bars), 2.4.1Δ*rpoH*$_{II}$ (dark gray bars), 2.4.1Δ*rpoH*$_{I}$ (light gray bars), and 2.4.1Δ*rpoH*$_{I}$ Δ*rpoH*$_{II}$ (white bars) was investigated under photooxidative stress. Relative expression was determined by real-time RT-PCR by using threshold cycle values obtained from RNA samples before and after 7 min of singlet oxygen exposure. For normalization, mRNA levels for *rpoZ* were used as an internal standard. Levels of significance are indicated as follows: ∗, $P \leq 0.01$; ∗∗, $P \leq 0.05$; and ∗∗∗, $P \leq 0.1$.

the observation that genes transcribed from an $RpoH_I/RpoH_{II}$ promoter are induced under $^1O_2$ as well as heat stress. Our findings clearly showed that the overlapping $RpoH_I$ and $RpoH_{II}$ regulons include noncoding sRNAs. This extends the functional role of genes controlled by the two RpoH sigma factors and suggests that sRNAs may be involved in posttranscriptional gene regulation in response to $^1O_2$ and heat in *R. sphaeroides*.

DISCUSSION

$RpoH_I$ and $RpoH_{II}$ control the heat and photooxidative stress responses. Increased temperatures in surface layers of, e.g., aquatic photic zone environments, microbial mats, and soils, are usually caused by high solar radiation. Hence, both stresses, heat and photooxidative stress, as caused by chlorophyll-mediated $^1O_2$ formation, are likely to occur simultaneously and may therefore be tightly linked in photosynthetic organisms. The idea that the regulatory response to $^1O_2$ and heat stress may overlap in *R. sphaeroides* is based on the findings that (i) the deletion of the gene encoding the heat shock-like sigma factor $RpoH_{II}$ leads to sensitivity against $^1O_2$ exposure (22) and that (ii) $RpoH_I$ and $RpoH_{II}$ recognize similar promoters *in vitro* (12). Our idea is supported by the severe phenotype of the *rpoH*$_I$ *rpoH*$_{II}$ deletion strain found under both stress conditions. Furthermore, we found that expression of several genes, e.g., *ompR*, RSP1948, and *hslO*, as well as the sRNAs RSs0680a, RSs2461, and RSs1543, depends on both $RpoH_I$ and $RpoH_{II}$ and that those genes are induced by photooxidative stress and heat.

Exclusive roles of $RpoH_I$ and $RpoH_{II}$. Despite the fact that both $RpoH_I$ and $RpoH_{II}$ contribute to the response to heat and $^1O_2$, each sigma factor has its exclusive role. After induction by RpoE, $RpoH_{II}$ is the main factor of the $^1O_2$ stress response, controlling at least 115 genes with specific binding sites and potentially more than 170 genes that are also recognized by $RpoH_I$. $RpoH_{II}$-specific target sites are not activated even after 10 min of heat stress, in contrast to genes preceded by a promoter also recognized by $RpoH_I$ (data not shown). The important role of $RpoH_{II}$ for the photooxidative stress response is also confirmed by the $^1O_2$-sensitive phenotype of

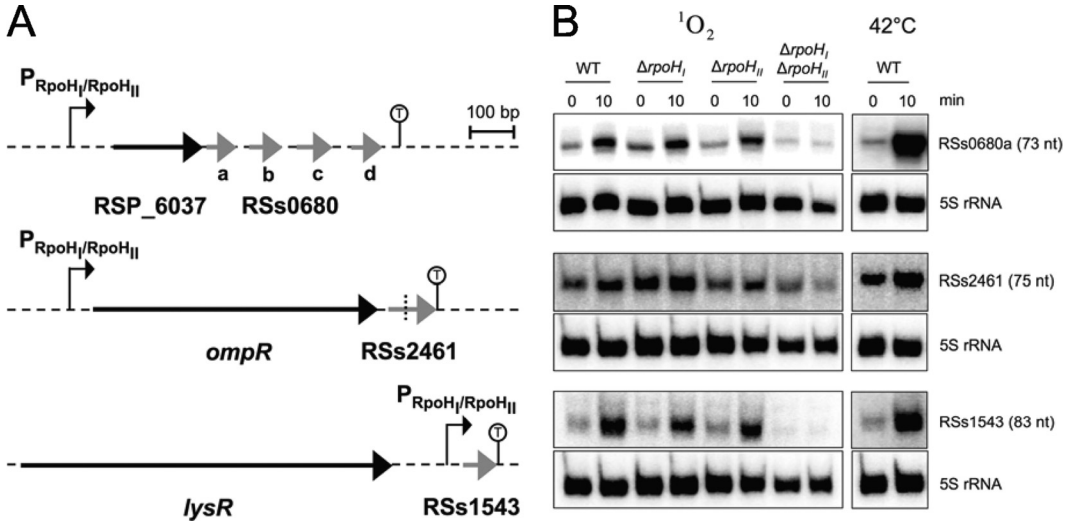

FIG. 6. Induction of RSs0680a, RSs2461, and RSs1543 under $^1O_2$ and heat stress depends on both $RpoH_I$ and $RpoH_{II}$. (A) The genetic localization of RSs0680a, RSs2461, and RSs1543 is depicted. RSs0680a and RSs2461 are transcribed together with the upstream gene from an $RpoH_I/RpoH_{II}$ promoter. RSs0680a is followed by three homologous sRNAs (RSs0680b to -d). RSs2461 is further processed after cotranscription (4), and the respective processing site is indicated by a dotted line. In contrast, RSs1543 is directly preceded by an $RpoH_I/RpoH_{II}$ promoter. A terminating structure is indicated by a stem-loop with a "T" in the loop. (B) Northern blot analysis of RSs0680a, RSs2461, and RSs1543. All three sRNAs are induced after 10 min of $^1O_2$ exposure in the wild-type (WT) and the *rpoH*$_I$ and *rpoH*$_{II}$ single-deletion strains. This induction is not observed in the *rpoH*$_I$ *rpoH*$_{II}$ deletion strain. After 10 min of heat stress, all three sRNAs are upregulated. In the case of RSs2461, only the 75-nt fragment is shown, which originates from a 116-nt precursor (4).

the *rpoH*$_{II}$ deletion strain (22) and the failure of RpoH$_{I}$ to fully compensate the lack of RpoH$_{II}$. In contrast, RpoH$_{II}$ is able to compensate the lack of RpoH$_{I}$ under $^{1}O_{2}$ stress, as the *rpoH*$_{I}$ deletion strain shows no significant change in $^{1}O_{2}$ sensitivity compared to that of the wild type. This indicates that most promoters recognized by RpoH$_{I}$ are also recognized by RpoH$_{II}$. The *rpoH*$_{I}$ *rpoH*$_{II}$ deletion strain is more sensitive to $^{1}O_{2}$ than the *rpoH*$_{II}$ deletion strain (Fig. 2); hence, RpoH$_{I}$ also contributes to the $^{1}O_{2}$ stress response but has most likely a minor role.

Our data demonstrate that RpoH$_{I}$ controls the heat stress response of *R. sphaeroides*, in contrast to earlier results showing that the deletion of *rpoH*$_{I}$ does not lead to a heat-sensitive phenotype in liquid cultures growing photosynthetically or by aerobic or anaerobic respiration (17). We now demonstrate that the *rpoH*$_{I}$ deletion strain is sensitive to heat when grown on malate minimal agar plates (Fig. 1). The *rpoH*$_{II}$ deletion strain was not affected and therefore, RpoH$_{I}$, but not RpoH$_{II}$, controls mainly the heat shock response in *R. sphaeroides*.

RpoH$_{II}$ target promoters differ from those recognized by both RpoH$_{I}$ and RpoH$_{II}$. In earlier work, we mapped the transcriptional start sites of selected RpoH$_{II}$-dependent genes to identify the corresponding putative target sequences. We found the highly conserved −10 element CTAGCT (22) that clearly differs from the respective elements in heat-inducible promoters recognized *in vitro* by both RpoH$_{I}$ and RpoH$_{II}$ (12).

To unravel what makes a target sequence specific for RpoH$_{II}$, we mapped the 5′ ends of further RpoH$_{II}$-dependent genes and additionally the 5′ ends of the *ompR* and RSP1948 mRNA, whose products are clearly dependent on both sigma factors. Obviously, the G in the CTAGVT motif allows recognition by only RpoH$_{II}$, whereas a T at this position leads to recognition by both factors. Interestingly, a variation of the −10 region motif comprised of CTAGSST was observed. Together with the finding that the MYATVT consensus is also recognized by RpoH$_{II}$, this leads to the conclusion that RpoH$_{II}$ is more flexible and recognizes a wider variety of −10 regions than RpoH$_{I}$. It is conceivable that distinct differences in the amino acid sequences of the region 2.4 of RpoH$_{I}$ and RpoH$_{II}$ (12), which is involved in the recognition of the −10 element, are responsible for the difference in promoter selectivity.

Redundancy in promoter elements of the regulatory response to photooxidative stress and heat. Several alphaproteobacteria that belong to the *Rhizobiales* and *Rhodobacterales* contain two or even three *rpoH* homologs in their genomes (12). Most likely, the additional heat shock sigma factors have been evolved by a gene duplication event and then diverged. Obviously, RpoH$_{II}$ of *R. sphaeroides* has been recruited for the response to $^{1}O_{2}$ and is controlled directly by RpoE, whereas RpoH$_{I}$ remained the major factor for the heat stress response. *Rhizobium etli* also harbors two heat shock-like sigma factors, RpoH1 and RpoH2. As in *R. sphaeroides*, they are able to complement a heat-sensitive *rpoH* deletion strain of *E. coli* and have different functions in *R. etli* (12, 20). RpoH1 is involved mainly in the heat shock and oxidative stress response, whereas RpoH2 participates in osmotic tolerance. In contrast to the *rpoH1* deletion strain, the *rpoH2* deletion strain is not negatively affected by heat shock, which is similar to *R. sphaeroides*. The *rpoH1 rpoH2* double-deletion strain shows the most severe phenotype to heat shock (20), which is in agreement with our studies for *R. sphaeroides*. The picture emerges that in the ancestors of the *Rhodobacterales* and *Rhizobiales* lineages, one of the *rpoH* copies was recruited for more specific functions. Together, the *rpoH* homologs appear to provide a balanced response to heat, oxidative and photooxidative stress, and changes in osmolarity and are involved in the interaction with other organisms (12, 20, 22). Other bacterial lineages also use redundancy in promoter elements to provide a balanced response to environmental changes. For example, in *E. coli*, the molecular basis of selective promoter recognition is known in detail for RpoD (σ^{70}) and RpoS (29). Here, a combination of exchanges in the single nucleotides in the −10 region and the nucleotides located between the −10 and −35 region that form either AT-rich stretches or an extended −10 element are important for the selectivity of the promoter. Furthermore, AT-rich stretches upstream of the −35 element bind further transcriptional regulators that affect sigma factor binding (30).

Bioinformatically predicted RpoH$_{II}$-dependent genes. In our bioinformatic search, we identified 115 genes preceded by a putative RpoH$_{II}$ promoter with a hexameric (CTAGVT) and/or a heptameric (CTAGSST) −10 element. We do not exclude the possibility that further genes preceded by very similar promoters may depend on RpoH$_{II}$. For example, in the upstream regions of the genes *gloB* (RSP0799) and *gpx* (RSP2389), we identified putative promoter sequences similar to those of the RpoH$_{II}$ promoter, with a heptameric motif in the −10 element. The putative promoter sequence CTG-N$_{18}$-CTATGAT is located 27 bp upstream of the translation start site of RSP0799, and a very similar sequence (TTG-N$_{18}$-CTATGCT) was identified 74 bp upstream of the translation start site of *gpx*. The *gloB* and *gpx* genes were shown previously to be dependent on RpoH$_{II}$ (22). In addition, we identified in our pyrosequencing approach several 5′ ends 5 to 10 bp downstream of putative −10 elements of promoters highly similar to those upstream of *gloB* and *gpx*. We therefore assume that the heptameric −10 element recognized by RpoH$_{II}$ is more variable than the hexameric −10 element. Also, the putative RpoH$_{I}$/RpoH$_{II}$ promoter upstream of the sRNA RSs1543, consisting of TTG-N$_{19}$-CTAAAT, shows a discrepancy to the RpoH$_{I}$/RpoH$_{II}$ promoter consensus motif KTG-N$_{(18–19)}$-MY ATVT. The RpoH$_{I}$/RpoH$_{II}$ regulon is likely to include even more genes, as identified by our bioinformatic search.

New functions in the response to $^{1}O_{2}$ exposure in *R. sphaeroides*. The response to $^{1}O_{2}$ requires DNA repair (2, 5), quinol oxidation, reduction of glutathione peroxide (5, 11), detoxification of methylglyoxal, $^{1}O_{2}$ scavenging (11, 22), glutathione (GSH)-dependent defense systems, protein turnover, export of small toxic waste products of biomolecules (ABC transporters), and scavenging of divalent metal ions (11).

Some of the genes identified by our bioinformatic prediction encode proteins which extend the functional response of *R. sphaeroides* to photooxidative stress known so far. Those proteins are involved in methionine sulfoxide reduction and aerobic respiration; homologs of RSP2617, a peptide methionine sulfoxide reductase, are involved in protection against oxidative stress in almost all organisms. Peptide methionine sulfoxide reductases catalyze the thioredoxin-dependent reduction of methionine sulfoxide (6, 19), which is generated by the reaction of methionine with reactive oxygen species, including $^{1}O_{2}$ (8).

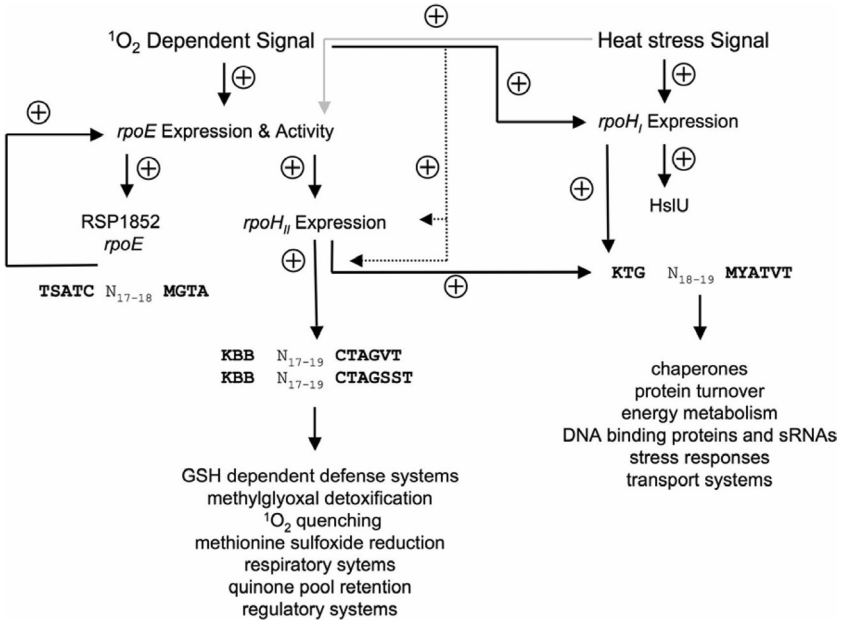

FIG. 7. Current model that displays the role of RpoE, $RpoH_I$ and $RpoH_{II}$ in the response to $^1O_2$ and heat stress in *R. sphaeroides*. Solid black arrows indicate strong positive effects in the regulatory cascade triggered by $^1O_2$ and heat stress. Solid gray arrows indicate less pronounced positive effects in the regulatory cascade. Dashed arrows indicate the function of hypothetical expression factors involved in the RpoE-$RpoH_{II}$-dependent gene induction. Representative promoter sequences for RpoE (2, 11) and the putative promoter consensus sequences for $RpoH_{II}$ or rather $RpoH_I$/$RpoH_{II}$ (Fig. 4B) are depicted. K: T or G; Y: T or C; B: T, C, or G; V: A, C, or G; M: C or A.

Some genes induced by $^1O_2$ exposure in an $RpoH_{II}$-dependent manner encode the following proteins that are involved in establishing and maintaining the respiratory system in the cell: QxtA (Rsp3213), the quinol oxidase I subunit; Cox15 (RSP3831), a putative cytochrome oxidase assembly factor; and Abc1 (RSP3305), a putative ubiquinol-cytochrome *c* reductase assembly protein belonging to the ABC1 family. The function of the respiratory chain is linked to the maintenance of an appropriate redox environment in the periplasm (3, 28). Induction of components of the respiratory pathway under photooxidative stress will keep the respiratory system functional after damages by $^1O_2$; otherwise, uncontrolled electron transfer from dehydrogenases to O_2 could lead to the formation of superoxide and hydrogen peroxide.

QxtA can counteract oxidative stress due to the maintenance of the quinone pool and its ability to limit accumulation of superoxide and peroxide by rapidly abstracting electrons from upstream dehydrogenases and transferring them to the oxidases (28). It was shown earlier that *qxtA* expression responds to redox alterations (21).

Furthermore, regulatory proteins encoded by the bioinformatically predicted genes could contribute to the photooxidative stress response. In this study and in earlier studies (11, 22), we observed proteins which are altered in synthesis upon $^1O_2$ exposure, but the respective genes are not preceded by a putative promoter recognized by RpoE, $RpoH_{II}$, or rather $RpoH_I$ and $RpoH_{II}$. The $RpoH_I$/$RpoH_{II}$-dependent regulatory proteins may contribute to the expression of those proteins and thereby extend the functional response to $^1O_2$.

Stress-inducible sRNAs extend the $RpoH_I$ and $RpoH_{II}$ regulons. The sRNAs RSs0680a, RSs2461, and RSs1543 are induced under $^1O_2$ and heat stress in an $RpoH_I$/$RpoH_{II}$-dependent manner. While we confirmed cotranscription of RSs0680a and RSs2461 together with their upstream genes, the sRNA RSs1543 is directly preceded by a conserved $RpoH_I$/$RpoH_{II}$ binding site. Similar to its paralog RSs2461, also RSs1543 is located next to a transcriptional regulator, maybe implying combined regulatory action. For RSs2461, which is cotranscribed with *ompR*, it has to be explored if this sRNA somehow regulates expression of *ompR* or if OmpR-regulated genes are regulated in concert with RSs2461. The low but detectable levels of *ompR* mRNA and RSs2461 sRNA in the $rpoH_I$ $rpoH_{II}$ deletion strain obtained with 5′-RACE and Northern blot experiments indicate recognition by an additional sigma factor such as, e.g., RpoD. In enterobacteria like *E. coli* or *Salmonella*, OmpR itself induces sRNAs like, e.g., MicC or MicF, which are regulators of the outer membrane protein composition (31). Targets of the $RpoH_I$/$RpoH_{II}$-dependent sRNAs of *R. sphaeroides* are not identified to date, and no function can be assigned. In our proteome analysis of the $^1O_2$-stressed $rpoH_I$ $rpoH_{II}$ deletion strain, we observed some protein spots, which are not present or less abundant in the stressed wild type. Somehow, the synthesis or stability of these proteins or the transcription of the respective genes is negatively affected by $RpoH_I$/$RpoH_{II}$. It is conceivable that the repression is due to (i) an $RpoH_I$/$RpoH_{II}$-dependent repressor or (ii) the action of the identified sRNAs.

Conclusion. Our current model (Fig. 7) shows in which manner the response to photooxidative stress and heat overlap in *R. sphaeroides* and thereby substantially extends previous models (22, 37). In brief, $^1O_2$ is recognized as a stress signal and increases the expression of *rpoE* and of those genes exhibiting a conserved RpoE promoter, including $rpoH_{II}$. Heat stress also triggers *rpoE* gene expression at a very low level. $RpoH_{II}$ con-

trols (i) genes specific to photooxidative stress and (ii) genes needed in the response to heat exposure by recognizing three different consensus target sites. Only one of those sites is also recognized by $RpoH_I$, which very likely regulates the heat response in concert with $RpoH_{II}$. Besides the RpoE promoter, the *rpoH*$_{II}$ gene putatively exhibits a second promoter recognized by itself and by $RpoH_I$ (see Table S4 in the supplemental material). This explains the low induction of the *rpoH*$_{II}$ gene in the *rpoE chrR* mutant strain TF18. More important, exposure to $^1O_2$ and heat triggers the expression of several regulatory factors, including DNA binding proteins and sRNAs. We assume that those factors are important for the regulatory control of genes not exhibiting an RpoE, $RpoH_{II}$, or $RpoH_I$/$RpoH_{II}$ promoter.

ACKNOWLEDGMENTS

We thank Monica Zobawa and Friedrich Lottspeich for identification of proteins by matrix-assisted laser desorption ionization–time of flight mass spectrometry (MALDI-TOF MS), Ulrike Ruppert for deletion of the *rpoH*$_I$ gene, and Johannes Schwarz for proteome analysis of the *rpoH*$_I$ deletion strains.

This project is funded by DFG grant Kl 563/20-1.

REFERENCES

1. **Anthony, J. R., J. D. Newman, and T. J. Donohue.** 2004. Interactions between the *Rhodobacter sphaeroides* ECF sigma factor, σ^E, and its anti-sigma factor, ChrR. J. Mol. Biol. **341:**345–360.
2. **Anthony, J. R., K. L. Warczak, and T. J. Donohue.** 2005. A transcriptional response to singlet oxygen, a toxic byproduct of photosynthesis. Proc. Natl. Acad. Sci. U. S. A. **102:**6502–6507.
3. **Bader, M., W. Muse, D. P. Ballou, C. Gassner, and J. C. Bardwell.** 1999. Oxidative protein folding is driven by the electron transport system. Cell **98:**217–227.
4. **Berghoff, B., A. J. Glaeser, C. Sharma, M. J. Vogel, and G. Klug.** 2009. Photooxidative stress-induced and abundant small RNAs in *Rhodobacter sphaeroides*. Mol. Microbiol. **74:**1497–1512.
5. **Braatsch, S., O. V. Moskvin, G. Klug, and M. Gomelsky.** 2004. Responses of the *Rhodobacter sphaeroides* transcriptome to blue light under semiaerobic conditions. J. Bacteriol. **186:**7726–7735.
6. **Brot, N., and H. Weissbach.** 2000. Peptide methionine sulfoxide reductase: biochemistry and physiological role. Biopolymers **55:**288–296.
7. **Cogdell, R. J., T. D. Howard, R. Bittl, E. Schlodder, I. Geisenheimer, and W. Lubitz.** 2000. How carotenoids protect bacterial photosynthesis. Philos. Trans. R. Soc. Lond. B Biol. Sci. **355:**1345–1349.
8. **Davies, M. J.** 2005. The oxidative environment and protein damage. Biochim. Biophys. Acta **1703:**93–109.
9. **Drews, G.** 1983. Mikrobiologisches Praktikum. Springer Verlag, Heidelberg, Germany.
10. **Glaeser, J., and G. Klug.** 2005. Photo-oxidative stress in *Rhodobacter sphaeroides*: protective role of carotenoids and expression of selected genes. Microbiology **151:**1927–1938.
11. **Glaeser, J., M. Zobawa, F. Lottspeich, and G. Klug.** 2007. Protein synthesis patterns reveal a complex regulatory response to singlet oxygen in *Rhodobacter*. J. Proteome Res. **6:**2460–2471.
12. **Green, H. A., and T. J. Donohue.** 2006. Activity of *Rhodobacter sphaeroides* $RpoH_{II}$, a second member of the heat shock sigma factor family. J. Bacteriol. **188:**5712–5721.
13. **Gross, C. A.** 1996. Function and regulation of the heat shock proteins, p. 1382–1399. *In* N. C. Neidhardt, R. Curtiss III, J. L. Ingraham, E. C. C. Lin, K. B. Low, B. Magasanik, W. S. Reznikoff, M. Rily, M. Schaechter, and H. E. Umbarger (ed.), *Escherichia coli* and *Salmonella*: cellular and molecular biology, 2nd ed., vol. 1. American Society for Microbiology, Washington, DC.
14. **Hendrischk, A. K., S. W. Frühwirth, J. Moldt, R. Pokorny, S. Metz, G. Kaiser, A. Jager, A. Batschauer, and G. Klug.** 2009. A cryptochrome-like protein is involved in the regulation of photosynthesis genes in *Rhodobacter sphaeroides*. Mol. Microbiol. **74:**990–1003.
15. **Hübner, P., J. C. Willison, P. M. Vignais, and T. A. Bickle.** 1991. Expression of regulatory *nif* genes in *Rhodobacter capsulatus*. J. Bacteriol. **173:**2993–2999.
16. **Janzon, L., S. Lofdahl, and S. Arvidson.** 1986. Evidence for a coordinate transcriptional control of alpha-toxin and protein-a synthesis in *Staphylococcus aureus*. FEMS Microbiol. Lett. **33:**193–198.
17. **Karls, R. K., J. Brooks, P. Rossmeissl, J. Luedke, and T. J. Donohue.** 1998. Metabolic roles of a *Rhodobacter sphaeroides* member of the sigma 32 family. J. Bacteriol. **180:**10–19.
18. **Keen, N. T., S. Tamaki, D. Kobayashi, and D. Trollinger.** 1988. Improved broad-host-range plasmids for DNA cloning in Gram-negative bacteria. Gene **70:**191–197.
19. **Levine, R. L., J. Moskovitz, and E. R. Stadtman.** 2000. Oxidation of methionine in proteins: roles in antioxidant defense and cellular regulation. IUBMB Life **50:**301–307.
20. **Martinez-Salazar, J. M., M. Sandoval-Calderon, X. Guo, S. Castillo-Ramirez, A. Reyes, M. G. Loza, J. Rivera, X. Alvarado-Affantranger, F. Sanchez, V. Gonzalez, G. Davila, and M. A. Ramirez-Romero.** 2009. The *Rhizobium etli* RpoH1 and RpoH2 sigma factors are involved in different stress responses. Microbiology **155:**386–397.
21. **Mouncey, N. J., E. Gak, M. Choudhary, J. Oh, and S. Kaplan.** 2000. Respiratory pathways of *Rhodobacter sphaeroides* 2.4.1: identification and characterization of genes encoding quinol oxidases. FEMS Microbiol. Lett. **192:**205–210.
22. **Nuss, A. M., J. Glaeser, and G. Klug.** 2009. $RpoH_{II}$ activates oxidative-stress defense systems and is controlled by RpoE in the singlet oxygen-dependent response in *Rhodobacter sphaeroides*. J. Bacteriol. **191:**220–230.
23. **Pappas, C. T., J. Sram, O. V. Moskvin, P. S. Ivanov, R. C. Mackenzie, M. Choudhary, M. L. Land, F. W. Larimer, S. Kaplan, and M. Gomelsky.** 2004. Construction and validation of the *Rhodobacter sphaeroides* 2.4.1 DNA microarray: transcriptome flexibility at diverse growth modes. J. Bacteriol. **186:**4748–4758.
24. **Pfaffl, M. W.** 2001. A new mathematical model for relative quantification in real-time RT-PCR. Nucleic Acids Res. **29:**e45.
25. **Prentki, P., A. Binda, and A. Epstein.** 1991. Plasmid vectors for selecting IS1-promoted deletions in cloned DNA: sequence analysis of the omega interposon. Gene **103:**17–23.
26. **Schilke, B. A., and T. J. Donohue.** 1995. ChrR positively regulates transcription of the *Rhodobacter sphaeroides* cytochrome c_2 gene. J. Bacteriol. **177:**1929–1937.
27. **Simon, R., M. O'Connell, M. Labes, and A. Puhler.** 1986. Plasmid vectors for the genetic analysis and manipulation of *Rhizobia* and other gram-negative bacteria. Methods Enzymol. **118:**640–659.
28. **Soballe, B., and R. K. Poole.** 2000. Ubiquinone limits oxidative stress in *Escherichia coli*. Microbiology **146**(Pt. 4)**:**787–796.
29. **Typas, A., G. Becker, and R. Hengge.** 2007. The molecular basis of selective promoter activation by the sigma(S) subunit of RNA polymerase. Mol. Microbiol. **63:**1296–1306.
30. **Typas, A., S. Stella, R. C. Johnson, and R. Hengge.** 2007. The −35 sequence location and the Fis-sigma factor interface determine sigmas selectivity of the *proP* (P2) promoter in *Escherichia coli*. Mol. Microbiol. **63:**780–796.
31. **Urban, J. H., and J. Vogel.** 2007. Translational control and target recognition by *Escherichia coli* small RNAs *in vivo*. Nucleic Acids Res. **35:**1018–1037.
32. **van Helden, J., B. Andre, and J. Collado-Vides.** 2000. A web site for the computational analysis of yeast regulatory sequences. Yeast **16:**177–187.
33. **van Niel, C. B.** 1944. The culture, general physiology, morphology, and classification of the non-sulfur purple and brown bacteria. Bacteriol. Rev. **8:**1–118.
34. **Vieira, J., and J. Messing.** 1982. The pUC plasmids, an M13mp7-derived system for insertion mutagenesis and sequencing with synthetic universal primers. Gene **19:**259–268.
35. **Wu, J., and A. Newton.** 1996. Isolation, identification, and transcriptional specificity of the heat shock sigma factor sigma32 from *Caulobacter crescentus*. J. Bacteriol. **178:**2094–2101.
36. **Zeller, T., and G. Klug.** 2004. Detoxification of hydrogen peroxide and expression of catalase genes in *Rhodobacter*. Microbiology **150:**3451–3462.
37. **Ziegelhoffer, E. C., and T. J. Donohue.** 2009. Bacterial responses to photooxidative stress. Nat. Rev. Microbiol. **7:**856–863.